Transactions of The Indian Institute of Metals
Vol. 62, Issues 4-5, August-October 2009, pp. 299-304

Simulation of microstructure formation in technical aluminum alloys using the multiphase-field method

B. Böttger, A. Carré, J. Eiken, G.J. Schmitz and M. Apel

ACCESS at the RWTH Aachen University, Intzestr. 5, D-52072 Aachen, Germany

E-mail : b.boettger@access.rwth-aachen.de

Received 07 August 2009
Revised 16 October 2009
Accepted 19 October 2009
Online at www.springerlink.com

Keywords:
aluminium alloys; multiphase-field; solidification; heat treatment; homogenization; microstructure; segregation simulation

Abstract

Simulation results of microstructure evolution in technical aluminum alloys are presented. The examples comprise solidification and further heat treatment of three different alloy classes, namely for the hypoeutectic alloy AA6061, the near eutectic alloy A356 and the highly alloyed, hypereutectic commercial alloy KS1295 being used in automotive applications. After a short introduction to the simulation models being applied - especially to the multiphase-field approach coupled to thermodynamic databases - the evolving microstructures are discussed in the context of the interplay between thermodynamics, kinetics, interfacial properties and nucleation.

Introduction

Microstructure simulation according to the phase-field method has now reached a level where the prediction of the microstructure evolution in technical alloys and under technical process conditions becomes possible. Microstructural parameters like the secondary dendrite arm spacing (DAS) or the size and nature of intermetallic precipitates are of primary importance for the mechanical properties of the cast product, and a realistic microstructure simulation approach including microsegregation patterns can help to optimize for example the alloy composition or conditions of the casting or homogenisation processes.

Crucial for the modelling of multicomponent and multiphase technical alloys is a proper description of the thermodynamic properties of the alloy. The CALPHAD approach [1,2] has proven to be very powerful for calculating phase equilibria in complex alloy systems. Databases for many important classes of technical alloys are available nowadays, see [3,4], compiling a vast quantity of experimental data in binary, ternary and higher order alloy systems.

A consequent continuation of this idea is the online coupling of such databases to the multiphase-field model by replacing the global equilibrium consideration with local equilibrium conditions. The first steps in this direction were made by coupling for example the thermodynamic software Thermo-Calc [3] to a multiphase-field model [5,8] using the TQ Fortran interface [6,7]. From these early models, the quasi-equilibrium approach was developed [8], which has been successfully applied to different material classes like steels [9], magnesium alloys [10,11] or superalloys [12], and which is implemented in the software package MICRESS® [13]. Comprehensive reviews about the coupling of thermodynamic data to phase-field models detail a number of different aspects [14-16].

In the field of aluminium alloys, there is a high interest in microstructure simulation originating from the automotive industry caused by a demand for lightweight alloys with optimized mechanical properties. Consequently, several approaches for the simulation of microstructure formation in technical aluminum alloys have been used so far, incorporating thermodynamic data on different levels [17-22]. In this paper, we are going to demonstrate the application of our multiphase-field model [5,8] with direct coupling to thermodynamic databases for different examples, namely the calculation of microsegregation in the hypoeutectic alloy AA6061, the widely used A356 casting alloy, and, finally, the slightly hypereutectic piston alloy KS1295. In the first case, microstructure details are not of primary interest, but the microsegregation of the alloying elements Si and Mg as well as the distribution of impurities of Fe and Cu after solidification are important for further homogenisation treatments. Accordingly, examples for the estimation of homogenisation times will be discussed. The second example details the simulation of microstructure evolution during sand casting of A356 starting from an experimentally determined temperature curve. For the rather low cooling rate typical for sand casting, the structure of the Al-Si eutectic can be resolved and the simulation provides an estimate of the lamellar spacing under realistic casting conditions. The third example depicts first results on microstructures comprising a large number of different intermetallic phases forming during solidification of the commercial alloy KS1295.

The Multiphase-Field Model

The multiphase-field theory describes the evolution of multiple phase-field parameters $\phi_a(\vec{x},t)$ in time and space. The phase-field parameters reflect the spatial distribution of

different grains of different orientation or of a number of phases N with different thermodynamic properties. At the interfaces, the phase-field variables change continuously over an interface thickness η which can be defined as being large compared to the atomic interface thickness but small compared to the microstructure length scale. The time evolution of the phases is calculated by a set of phase-field equations deduced by the minimization of the free energy functional [5,8]:

$$\dot{\phi}_\alpha = \sum_\beta M_{\alpha\beta}(\vec{n})\left(\sigma^*_{\alpha\beta}(\vec{n})\,K_{\alpha\beta} + \tfrac{\pi}{\eta}\sqrt{\phi_\alpha\phi_\beta}\;\Delta G_{\alpha\beta}(\vec{c},T)\right) \qquad (1)$$

$$K_{\alpha\beta} = \phi_\beta\nabla^2\phi_\alpha - \phi_\alpha\nabla^2\phi_\beta + \frac{\pi^2}{\eta^2}\left(\phi_\alpha - \phi_\beta\right) \qquad (2)$$

In equation (1), $M_{\alpha\beta}$ is the mobility of the interface as a function of the interface orientation, described by the normal vector $\vec{n}$ $\sigma^*_{\alpha\beta}$ is the effective anisotropic surface energy (surface stiffness), and $K_{\alpha\beta}$ is related to the local curvature of the interface. The interface, on the one hand, is driven by the curvature contribution $\sigma^*_{\alpha\beta}K_{\alpha\beta}$ on the other hand by the thermodynamic driving force $\Delta G_{\alpha\beta}$. The thermodynamic driving force, which is a function of temperature T and local (multicomponent) composition $\vec{c}$, couples the phase-field equations to the diffusion equations

$$\dot{\vec{c}} = \nabla\sum_{\alpha=1}^{N}\phi_\alpha\vec{D}_\alpha\nabla\vec{c}_\alpha \qquad \text{with } \vec{c} \text{ defined by } \vec{c} = \sum_{\alpha=1}^{N}\phi_\alpha\vec{c}_\alpha \qquad (3)$$

and $\vec{D}_\alpha$ being the multicomponent diffusion coefficient matrix for phase α. $\vec{D}_\alpha$ is calculated online from databases for the given concentration and temperature.

The above equations are implemented in the software package MICRESS® [13] being used for the simulations throughout this paper. Direct coupling to thermodynamic and mobility databases is accomplished via the TQ-interface of Thermo-Calc Software [3]. The thermodynamic driving force ΔG and the solute partitioning are calculated separately using the quasi-equilibrium approach [8], and are introduced into the equation for the multiple phase-fields (Equation 1). This allows the software package to be highly flexible with respect to thermodynamic data of a variety of alloy systems and not to be restricted by the number of elements or phases being considered. A multi-binary extrapolation scheme [8] has been implemented in order to minimize the thermodynamic data handling, especially for complex alloy systems.

Further material data as for example interfacial energies, interface mobilities or nucleation conditions are not available from databases so far and have to be calibrated on the basis of experimental results instead, like for example grain sizes or precipitate distributions, or they even have to be estimated. Subsequent to such a calibration for a given alloy system, parameter variations with a predictive character become possible.

Simulation Results for AA6061

AA6061 is one of the most common aluminum alloys. Its applications range from construction of aircraft structures to automotive parts as well as motorcycle or bicycle frames. Several reasons account for the popularity of this alloy. The A6061 shows good corrosion resistance at both atmospheric and sea water conditions. Moreover, A6061 can be easily welded and has interesting machinability and formability characteristics. These positive features, however, strongly depend on the heat treatment procedure as A6061 is a precipitation hardening alloy and the intermetallic precipitates block dislocation movement. The density and size of these intermetallics are a result of the subtle interplay between kinetics and thermodynamics.

For the present study we selected an A6061 aluminum alloy with the following composition (in wt%): Al: (bal) Mg: 1.0 Si: 0.725 Fe: 0.315 and Mn: 0.114 .

The databases used for the simulations were the COST 507 light alloy thermodynamic database [23] and the mobAl1 mobility database [24]. Initial thermodynamic equilibrium and Scheil-Gulliver calculations using Thermo-Calc predicted the following sequence of phases appearing during the solidification of this alloy: liquid, fcc-Al , $Al_{13}Fe_4$, α-AlFeSi, β-AlFeSi, Mg_2Si, α-AlMnSi, δ-AlMnSi and Si. All these phases were taken into account for the MICRESS® simulation.

The simulation domain had a size of 150 x 150 micrometers with a grid spacing of 1μm. The interface mobility of the fcc-Al phase was calibrated to ensure a diffusion-controlled growth, the interface mobilities of the intermetallics as well as the nucleation scheme were calibrated to be consistent with experimental data [25,26]. The mobilities of the α-AlFeSi/liquid and β-AlFeSi/liquid interfaces and the nucleation undercoolings for example were calibrated in order to quantitatively reproduce the α-AlFeSi/β-AlFeSi ratio reported by Tanihata [27] during the solidification stage. For AA6061 a seed undercooling scenario was used and seeds were placed at the interface liquid/fcc-Al when a critical undercooling ΔT was locally reached. ΔT values of 4K, 30K and 10K were set for nucleation of the Si, α-AlFeSi and Mg_2Si phases on fcc-Al, respectively. In this context also effects evoked by the curvature of the alpha-Al interface were considered. Nucleation of β-AlFeSi was assumed to occur at the interface between liquid and α-AlFeSi with a critical undercooling of 10K

Interfacial energies were set to 10^{-4} J/cm^2 for the liquid/silicon and liquid/intermetallics interfaces and to 10^{-3} J/cm^2 for the fcc/silicon and fcc/intermetallics interfaces. The liquid/fcc interfacial energy was adopted from Kurz-Fisher [28] to be $1.6*10^{-5}$ J/cm^2 .

In order to efficiently simulate microsegregation and to spatially resolve the individual phases, only a quarter of a grain was simulated without loss of information due to symmetry considerations. The dendrite trunk of this grain was set to grow diagonally according to a unit cell model with periodic or symmetric boundary conditions. The solidification of the alloy was then simulated using a constant heat extraction rate of 20 W/cm^2, resulting in a total solidification time of 70s.

According to experimental observations [25,27], α-AlFeSi appears during cooling via the solidification reaction:

$$L \rightarrow \alpha\text{-AlFeSi} + \text{fcc-Al}$$

During the subsequent peritectic reaction

$$L + \alpha\text{-AlFeSi} \rightarrow \beta\text{-AlFeSi} + L + \text{fcc-Al}$$

the β-AlFeSi intermetallic partially nucleates on the α-AlFeSi. The resulting phase distributions, Fig. 1, and microsegregation patterns were subsequently used as input

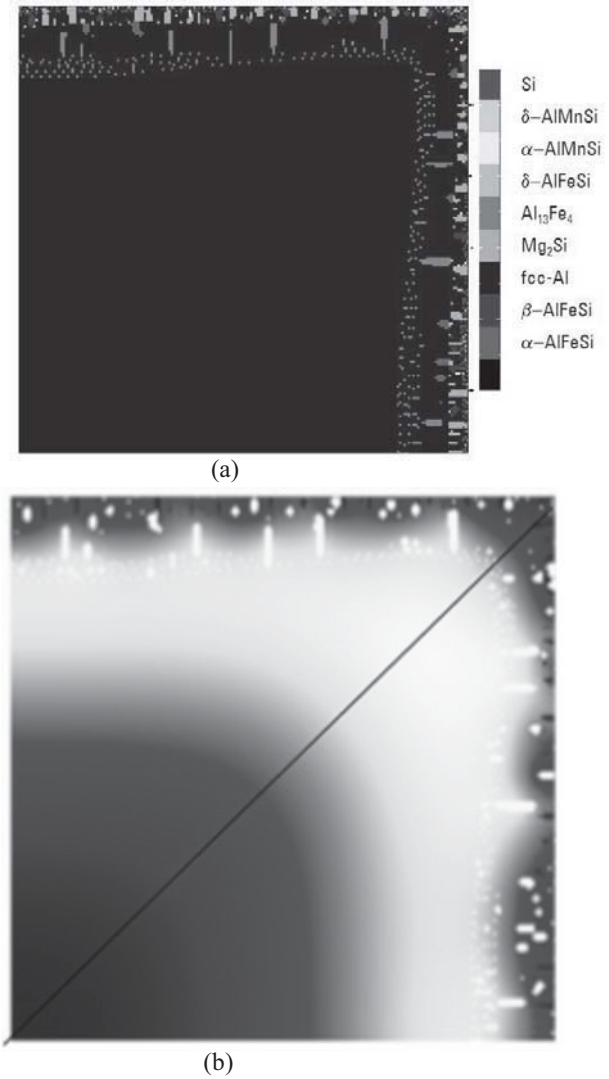

Fig. 1 : Distribution of phases after solidification of AA6061 in the unit cell model (a). The simulation domain (150 μm*150 μm) corresponds to a quarter of a grain, which grew from the lower left to the upper right. The diagonal thus corresponds to 50% of the grain diameter as determined from experiments. Different types of intermetallic precipitates are indicated by different colors. (b): Color representation of Fe distribution after approx. 2h of heat treatment at 580°C. The diagonal black line indicates the line scan for quantitative element profiles shown in figures 2b and 2c.

data for a simulation of a homogenization heat treatment for up to sixteen hours at 580°C. Microsegregation patterns, Fig. 2, and phase distributions were recorded after 7300, 17300, 27300, 37300, 47300 and 57300s of numerical heat treatment (i.e. after approx. 2h, 5h, 8h, 10h, 13h and 16h). More details, especially with respect to the evolution of the ratio β-AlFeSi/α-AlFeSi, which is a result of a complex interplay of nucleation and peritectic reactions during solidification and a peritectoid transformation during homogenization, will be discussed in relation to expected equilibrium phase fractions and will be published elsewhere [29].

Simulation Results for A356

Simulation of the solidification of A356 was performed for the following alloy composition (in wt.%): Al (bal.), Si: 7.08

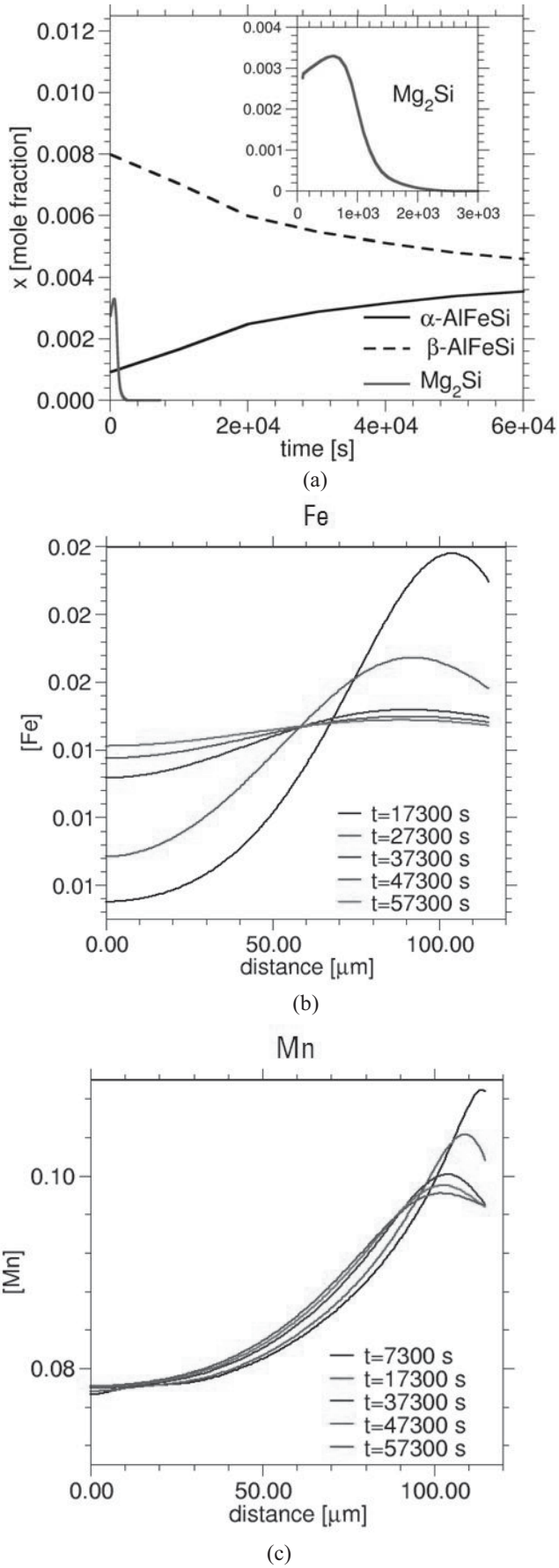

Fig. 2 : Evolution of the minority phase fractions during heat treatment at 580^0C(a) and evolution of the segregation along the line scan (see fig. 1b) in wt% for Fe (b) and Mn (c) for different heat treatment times. While the Fe distribution is almost homogenous after 16h, the Mn distribution is not homogeneous at all.

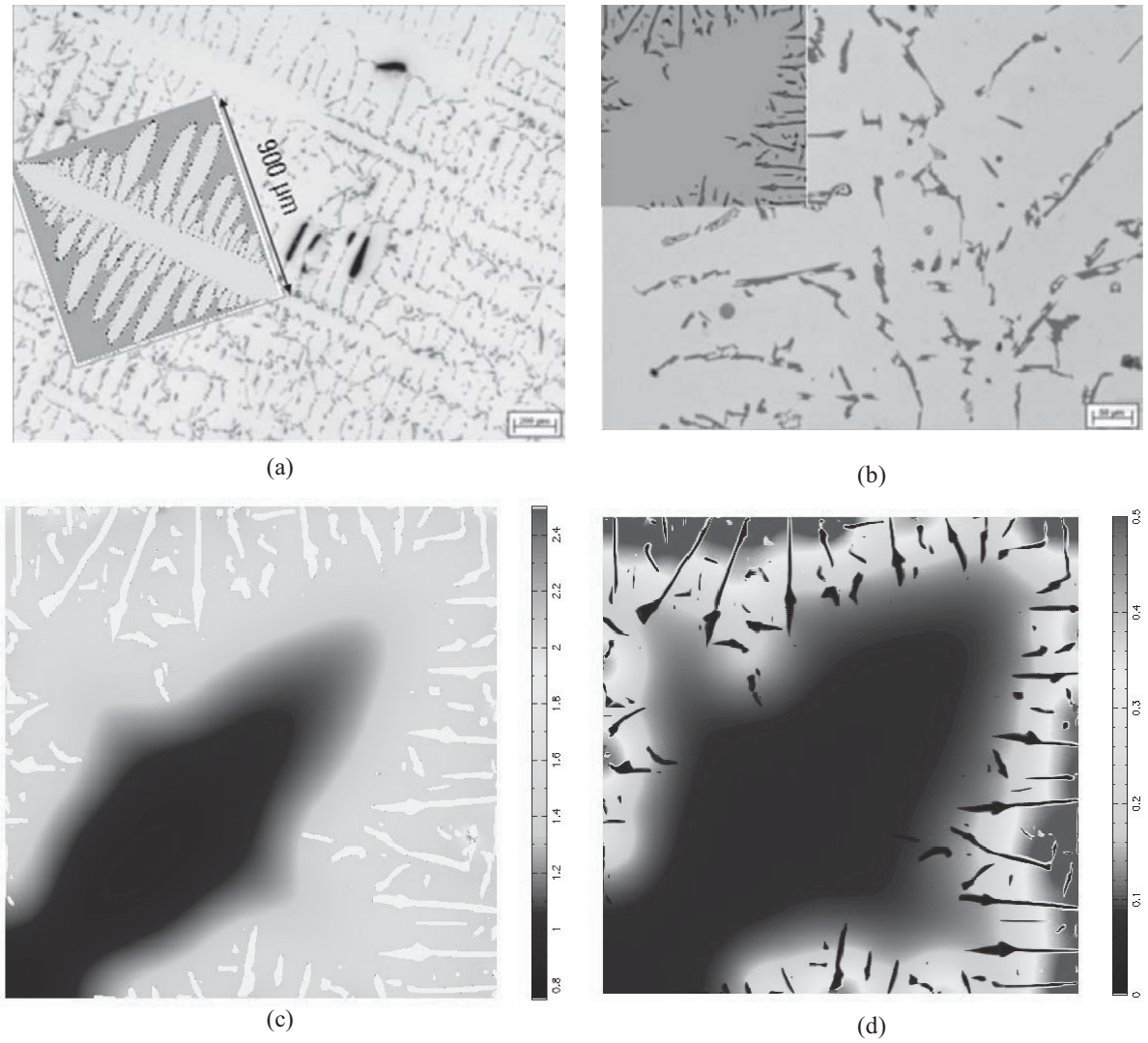

Fig. 3 : Comparison of simulated structures with experimental structures. The simulated DAS ((a)-insert) qualitatively compares rather well with experimental DAS (87±16 µm) (a). Also the size and the structure of the silicon lamellae show good qualitative agreement between experimental observations (b) and simulations (b, insert). The corresponding microsegregation patterns, being highly important for subsequent homogenization heat treatments, are shown for Si (c) and Mg (d) with concentrations depicted in wt.%. The size of the simulation domain is 240µm by 240 µm for (b,insert) and (c) and (d).

and Mg: 0.3. As for AA6061, the COST507 and mobAl1 databases were used. Following phases were considered in the simulations: liquid, fcc-Al, Si and Mg_2Si. Interfacial properties and nucleation conditions were selected according to the AA6061 example.

The typical length scales observed in the microstructure after sand casting of this alloy span a wide range: grain sizes of several mm, secondary dendrite arm spacings of approx 50 to 100µm and precipitate sizes of 2µm to 100µm (for Si - precipitates) down to 10nm to100µm (for Mg_2Si-precipitates) are of relevance.

Accordingly, the simulation of this microstructure is a multiscale problem, and size and resolution of the simulation domain have to be selected according to the morphology details of interest. In order to simulate the DAS, the experimental grain size (~ 3mm dia.) was again used as an input for a unit cell model. Experimental values for the heat-flux derived from thermocouple readings were taken as a heat-flux boundary condition for the temperature calculation following a heat balance approach.

Simulation of solidification in a unit cell under these conditions yields a DAS value of 102 ± 28 µm being compatible with the experimental findings within the error bars, Fig 3a. The grid resolution used for these DAS simulations was Δx=1.5µm and further refined to Δx=200 nm to simulate the evolution of interdendritic precipitates and silicon lamellae, respectively, Fig 3b. Again the size of the silicon lamellae was qualitatively reproduced by the simulation, however their growth was almost perpendicular to the dendrite side arms, which has not been observed in experimental micrographs. Possible reasons are 2D/3D effects evoked by free flowing Si particles in the melt, which will be investigated in the future.

Simulation Results for KS 1295

KS 1295 is an industrial aluminium alloy for automotive pistons. It is slightly hypereutectic in Si and, furthermore, contains considerable amounts of Cu, Ni, Fe, Mg, Mn and Zn. Castings made of this alloy benefit from hardening by primary and eutectic silicon particles and by a big amount of various intermetallic precipitates. The amount, nature and morphology of these intermetallics are of high importance for the mechanical properties of the pistons which have to withstand the increasing loading pressures in modern diesel

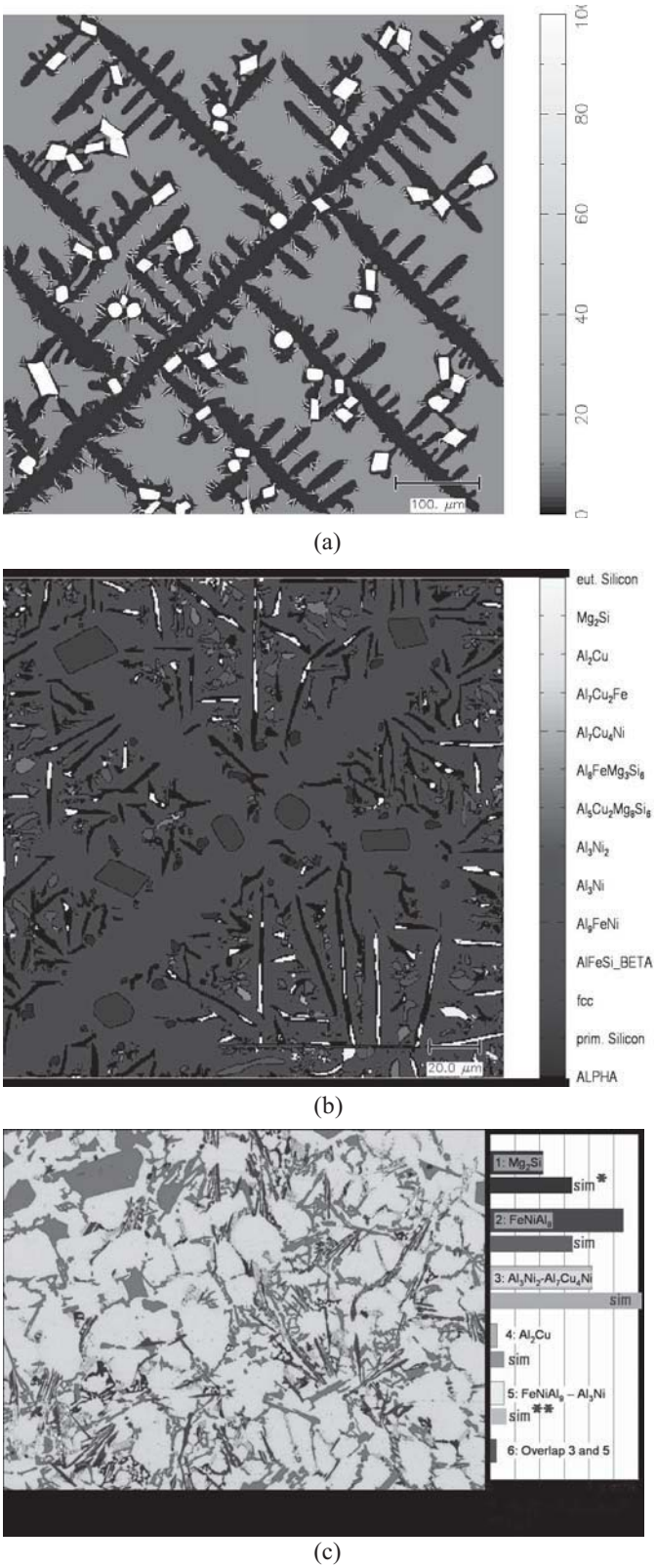

Fig. 4 : Comparison of simulated KS1295 microstructure with optical metallography. a) Simulated silicon concentration map of the first stage of solidification, showing big primary silicon particles getting overgrown by the fcc-Al dendrite as well as small eutectic silicon lamellae. b) Simulated distribution of the 14 different phases involved after complete solidification. c) Experimental microstructure map where part of the intermetallic phases have been identified or attributed to phase groups (courtesy of S. Barnes, University of Manchester). Experimental and simulated phase fraction (4c, right) are in good agreement.

engines.

The simulation shown is based on the TTAL5 [30] and mobAl1 [24] databases which provide the thermodynamic and diffusion data. The seven alloying elements given above were taken into account. As in the case of the AA6061 and A356 alloys, a unit cell approach based on a quarter of an equiaxed grain was used. However, in the case of the high-alloyed KS1295, the assumption of a given external heat extraction from the unit cell volume and the neglection of thermal gradients would lead to an unrealistically high recalescence effect not observed in technical castings and strongly affect the precipitation sequence of the intermetallic phases. Therefore, an iterative homoenthalpic approach was used which allows to simultaneously calculate the macroscopic temperature field in the vicinity of the microscopic simulation domain and the microstructure formation process in a consistent way [31].

Due to the complexity of the KS1295 alloy a number of unknown physical parameters had to be estimated in accordance to the microstructures observed experimentally. The interfacial energies between liquid and fcc, the intermetallic phases and silicon were estimated similarly as in the examples above. Nucleation of intermetallics was assumed to occur at the liquid-fcc interface with a typical critical undercooling of 15 K, a value of 25 K was chosen for silicon. The primary phases alpha and silicon were also nucleated directly from the melt using a seed-density model for heterogeneous nucleation [20] with a seed distribution recovering the experimentally observed abundance of the respective phases.

Figure 4a shows the silicon concentration distribution in wt% during the initial solidification stage, according to the phase-field simulation. Even though silicon is the primary phase which forms before nucleation of fcc-aluminium phase, the latter still is growing with a pronounced dendritic morphology being consistent with experimental findings. The reason for this behaviour is the high nucleation barrier for fcc-Al on the primary silicon particles which does not favour eutectic growth morphologies. The dendrite side branches are attracted by Si depletion around the primary particles, which therefore get entirely overgrown. Nucleation of secondary silicon occurs with an irregular eutectic morphology.

During further solidification more and more different intermetallic phases nucleate, and at the end of solidification as many as 14 phases have formed, Fig. 4b. Some of these phases have only small volume fractions and are hidden by the black interface regions. For comparison, an experimental micrograph of KS1295 is shown which was provided by Simon Barnes, University of Manchester. Sophisticated image analysis was performed allowing the assignment of the observed precipitates to phases or phase groups, Fig. 4c. A qualitative agreement between the simulated and measured microstructures was found. In a 2D simulation the growth of the fcc-Al dendrite by definition is restricted to the 2D plane. A quantitative comparison of experimental and simulated morphologies must however take 3D effects into consideration. Further details will be published elsewhere [32].

Conclusion and Outlook

Simulations on solidification and heat treatment of three different technical aluminum alloys were performed using the multiphase-field model and data available from commercial

thermodynamic and mobility databases. Further material data – especially the properties of the interfaces - were calibrated on the basis of experimental results or estimated. On the basis of the available data, estimates and calibrations, the simulated microstructures show good agreement with experimental observations in terms of similar length scales for dendrite arm spacings (DAS), sizes of silicon lamellae, amount and distribution of intermetallic phases and microsegregation patterns. Deviations from experimental results in terms of a quantitative comparison may be attributed to 3D effects in the 2D simulations or other phenomena, like fluid flow, not being considered by now.

The present and future benefits to be drawn from microstructure simulations range from the optimization of heat treatment schemes to the virtual development of new alloys, including a prediction of their effective materials properties by virtual testing [33]. In the long term, a simulation of process chains, comprising several steps like casting, heat treatment and subsequent operation and moreover bridging several length scales on the basis of a standardized virtual platform for materials processing [34], may eventually enable a life-cycle modelling of components and products.

Acknowledgments

The present work depicts results originating from a number of different projects, being supported by the German Research Society DFG under grant No. AP196//1 and by Kolbenschmidt-Pierburg AG. Their support is gratefully acknowledged.

References

1. http://www.calphad.org
2. Saunders N and Miodownik A, CALPHAD calculation of phase diagrams: a comprehensive guide. Elsevier; 1998.
3. Thermo-Calc Software: http://www.thermocalc.com
4. ThermoTech: http://www.sentesoftware.co.uk
5. Steinbach I, Pezzolla F, Nestler B, Seeßelberg M, Prieler R, Schmitz G J and Rezende J L L, A phase field concept for multiphase systems. *Physica D,* **94** (1996) 135.
6. Grafe U, Böttger B, Tiaden J and Fries S G, Coupling of Multicomponent Thermodynamic Databases to a Phase Field Model: Application to Solidification and Solid State Transformations of Superalloys, *Scripta Materialia,* **42**(12) (2000) 1179.
7. Böttger B, Grafe U, Ma D and Fries S G, *Mater. Sci. Technol.,* **16** (2000) 1425.
8. Eiken J, Böttger B and Steinbach I, Multiphase-field approach for multicomponent alloys with extrapolation scheme for numerical application, *Phys. Rev. E,* **73** (2006) 066122.
9. Böttger B, Apel M, Eiken J, Schaffnit P and Steinbach I, Phase-field simulation of solidification and solid-state transformations in multicomponent steels, *Steel Research Int.,* **79**(8) (2008) 608.
10. Eiken J, Böttger B and Steinbach I, Simulation of Microstructure Evolution during solidification of Magnesium-Based Alloys, *Trans. Indian Inst. Met.,* **60**(2-3) (2007) 179.
11. Böttger B, Eiken J, Ohno M, Klaus G, Fehlbier M, Schmid-Fetzer R, Steinbach I and Bührig-Polaczek A, Controlling microstructure in magnesium alloys: a combined thermodynamic, experimental and simulation approach. *Adv. Eng. Mater.*, **8** (2006) 241.
12. Warnken N, Ma D, Mathes M and Steinbach I, Investigation of eutectic island formation in SX superalloys, *Materials Science and Engineering A*, **413**(12) (2005) 267.
13. MICRESS®-the MICRostructure Evolution Simulation Software: www.micress.de
14. Steinbach I, Böttger B, Eiken J, Warnken N and Fries S G, CALPHAD and Phase-Field Modeling: A Successful Liaison, *Journal of Phase Equilibria and Diffusion,* **28**(1) (2007) 101
15. Kitashima T, Coupling of the phase-field and CALPHAD methods for predicting multicomponent solid-state phase transformations, *Phil. Mag.*. **88**(11) (2008) 1615.
16. Fries S G, Böttger B, Eiken J and Steinbach I, Upgrading CALPHAD to microstructure simulation: the phase-field method, *Int. J. Mat. Res.*, **100** (2009) 2
17. Qin R S, Wallach E R and Thomson R C, A phase-field model for the solidification of multicomponent and multiphase alloys, *J. Cryst. Growth*, **279**(1-2) (2005) 163
18. Kovacevic I, Simulation of spheroidisation of elongated Si-particle in Al-Si alloys by the phase-field model, *Mater. Sci. Eng. A,* 496(1-2) (2008) 345
19. Wang J S and Lee P D, Quantitative Simulation of Fe-rich Intermetallics in Al-Si-Cu-Fe Alloys during Solidification, Proceedings of 138th TMS Annual Meeting and Exhibition, San Francisco Feb 2009, VOL 1: Materials Processing and properties
20. Böttger B, Eiken J and Steinbach I, Phase field simulation of equiaxed solidification in technical alloys, *Acta Mater.,* **54** (2006) 2697.
21. Böttger B, Apel M, Barnes S, Scheppe F and Sagel A, Computer Aided Development of Improved Alloys for Automotive Pistons, presentation at the 11th International Conference on Aluminium Alloys ICAA Neckarsulm (Germany), (2008)
22. Qin R S, Wallach E R, A phase-field model coupled with a thermodynamic database, *Acta Mat.* **51**(20) (2003) 6199
23. COST 507 Thermochemical database for light metal alloys, Vol.2, Eds. I.Ansara, A.T.Dinsdale, M.H.Rand, Publications of the European Communities, Luxembourg, 1998 (ISBN 92-828-3902-8). Database available e.g. from [3]
24. MOBAL1: Mobility database for Al-alloys, Thermo-Calc Software: www.thermocalc.se
25. Sha G K A, O'Reilly Q, Cantor B, Worth J and Hamerton R, Growth Related metastable phase selection in A 6XXX series wrought Al alloy, *Mat. Sci. Eng. A,* **304-306** (2001) 612.
26. Samaras S N, Modelling of microstructure evolution during precipitation processes: a population balance approach of the KWN model, *Modelling and Simulation in Materials Science and Engineering,* **14**(8) (2006) 1271
27. Tanihata H, Sugawara T, Matsuda K and Ikeno S, *Journal of Materials Science,* **34** (1999) 2105.
28. Kurz-Fisher, Fundamentals of Solidification; Trans Tech Publications (1989)ISBN 0-87849-522-3
29. Carré A, et al., to be published
30. TTAl5: thermodynamic database for Aluminum alloys developed by [4]
31. Böttger B, Eiken J and Apel M, Phase-field simulation of microstructure formation in technical castings – A self-consistent homoenthalpic approach to the micro–macro problem, *J. Comput. Phys.* (2009) 6784
32. Böttger B, et al., to be published
33. Apel M, Benke S and Steinbach I, Virtual Dilatometer Curves and effective Young's modulus of a 3D multiphase structure calculated by the phase-field method, *Computational Materials Science,* **45** (2009) 589
34. G.J.Schmitz and U.Prahl: Toward a Virtual Platform for Materials Processing, *JOM*, **61**(5) (2009)19